International Journal of Modern Physics C, Vol. 9, No. 3 (1998) 409–419

A MONTE CARLO SIMULATION OF AN IN-PLANE SWITCHING LIQUID CRYSTAL DISPLAY

CESARE CHICCOLI* and PAOLO PASINI†
Istituto Nazionale di Fisica Nucleare, Sezione di Bologna
Via Irnerio 46, 40126 Bologna, Italy
**E-mail: chiccoli@bo.infn.it*
†*E-mail: pasini@bo.infn.it*

STEFANO GUZZETTI and CLAUDIO ZANNONI‡
Dipartimento di Chimica Fisica ed Inorganica dell' Università
Viale Risorgimento 4, 40136 Bologna, Italy
‡*E-mail: vz3bod7a@sirio.cineca.it*

Received 20 January 1998
Revised 27 February 1998

The Monte Carlo (MC) method is applied to the modeling of a liquid crystal display based on the in-plane switching effect. This is the first attempt to simulate this device features starting from purely microscopic molecular interactions. The optical textures are obtained from the Monte Carlo generated microscopic equilibrium configurations by means of a Müller matrix approach. Suitable order parameters are also calculated to quantify the ordering and the molecular organization across the display cell.

Keywords: Computer Simulations; Liquid Crystals; Displays; Monte Carlo.

1. Introduction

Metropolis Monte Carlo (MC) simulations have been widely applied in studying the Physics of Liquid Crystals.[1–12] In particular a significant amount of work has been done in investigating their bulk thermodynamic and ordering properties[1–7] and, more recently, the numerous phenomena connected to their confinement.[8–12] However, the MC technique is potentially very powerful in a much broader range of applications as it allows the modeling of the effect of various combined microscopic and macroscopic factors, such as boundary conditions, anchoring strength, temperature, external applied fields, etc., on the molecular organization of nematic electro-optical systems.

Recently we have applied this technique to simulate a model of a twisted nematic (TN) display[12] starting from a very simple intermolecular potential used to describe the nematic liquid crystal orientational behavior.

Here we wish to present a Monte Carlo simulation of the recently proposed and not so well understood *in-plane switching* LC display.[13,14]

In this device the top and bottom transparent cell surfaces are treated to induce homogeneous, i.e., surface parallel, alignment along the same direction (x in Fig. 1). A polarizer and an analyzer, with orthogonal polarization directions (for example along the x and y axis) are placed respectively above and below the cell. Thus a display element, say a pixel, does not let light through with no field applied and is black. Contrary to the twisted nematic case, the liquid crystalline material filling the cell is chosen to have a negative dielectric anisotropy. The lateral switching effect is due to the application of an external electric field (see Fig. 1) across two electrodes placed at a certain distance from the surfaces and in a plane orthogonal to the light direction. The field is applied across the cell, and ideally it acts only on the molecules belonging to a thin intermediate layer of the liquid crystal sample. Notice that the direction of the applied field is parallel to the surface alignment direction but, due to the negative dielectric anisotropy, the molecules subjected to the field tend to rotate by 90 degrees so that a twisted alignment is induced between this intermediate layer and the two aligned surfaces.

Contrary to the usual twisted nematic display the light is thus transmitted only where the effect of the field is sufficiently strong and the background of the image is black.

A schematic representation of the in-plane liquid crystal display operation mode is shown in Fig. 1.

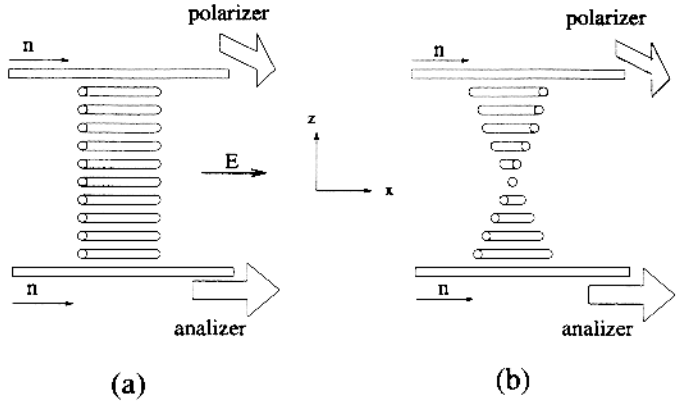

Fig. 1. A sketch of the operation mode of the In-Plane Switching LC display with the light propagation direction along the z axis. The alignment direction of the surfaces is indicated by **n**. (a) Field off: the polarized light is not transmitted through the cell; (b) Field on: a layer of nematic molecules rotates and the director twist changes the polarization of the incoming light which now passes through the analyzer.

2. The Simulations

Our display simulation is based on the Lebwohl–Lasher (LL) lattice spin model[1] where each three-dimensional spin represents a molecule or, more appropriately, a closely packed group of molecules that maintains its short range order across the

nematic-isotropic phase transition.[9] A system of N such pseudoparticles, placed on the sites of a cubic lattice has the Hamiltonian

$$U_N = -\sum_{\substack{i,j \\ i<j}} \epsilon_{ij} P_2(\cos\beta_{ij}) - J\epsilon\xi \sum_i P_2(\cos\varphi_i)\,, \tag{1}$$

where the first term is the LL potential with ϵ_{ij} a positive constant giving the interaction strength, ϵ, for nearest neighbor particles i and j and zero otherwise, β_{ij} is the angle between the axis of the two molecules, P_2 is a second rank Legendre polynomial. This LL model reproduces satisfactorily the orientational behavior of a nematic liquid crystal in the bulk and the phase transition to an isotropic phase.[1–5]

The second term on the right hand side of Eq. (1) models at the microscopic level the application of an external field. Here φ_i is the angle between the field direction and the symmetry axis of particle i, ξ determines the sign and strength of coupling with the field $\mathbf{E}$ while the parameter $J = 1$ or 0 acts as a switch to turn on or off the external field. The strength of interaction of the system with the electric field $\mathbf{E}$, denoted in our model by the parameter ξ, is in reality macroscopically described by the dielectric anisotropy $\Delta\epsilon$.

To mimic the alignment of the nematic at the cell surfaces we have imposed a fixed orientation along x to the spins belonging to the top and bottom layers of the lattice. Periodic boundary conditions are instead employed around the four other faces of the simulation box.

The external field, directed along the x axis, is applied only to an intermediate layer. To mimic the effect of an array of addressable electrodes, this layer is further divided in a regular array of domains where the field can operate (ON) or not (OFF). In this way it is possible to control the effect of the local field to produce a desired pattern.

The initial configuration of the nematic spin system is chosen at random or from a completely ordered one and we have used a standard Metropolis algorithm[15] to update the lattice choosing a particle at random and varying the spin orientation. To maintain an acceptance ratio of about 50%, we have implemented a Barker–Watts[16] evolution with a controlled angular displacement. After equilibrium is reached we start to accumulate averages of interesting observables such as, for example, order parameters and to calculate the optical pattern corresponding to the chosen active electrode configuration. We have performed simulations on $10 \times 10 \times 10$ and $50 \times 30 \times 10$ lattices at selected temperatures in the nematic phase. We have used at least 20 000 and 10 000 cycles for equilibration and production respectively, where we call a cycle a set of N attempted moves.

To perform simulations of these system sizes we have used HP 755 and DEC AXP 7000-710 type platforms. We recall that the main purpose of the present work was to investigate the response of the in-plane alignment induced in a lattice model. As we will show in the next sections the results are very encouraging and the use of more powerful computers or special purpose platforms[7] will allow us to perform more

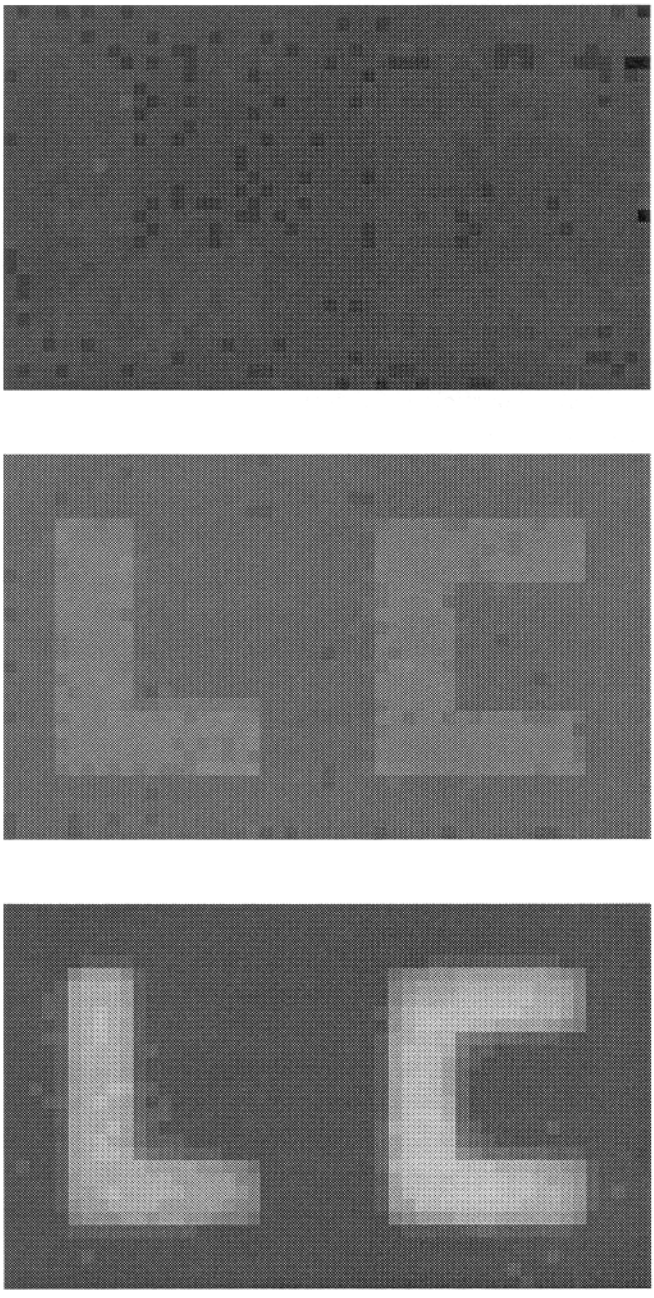

Fig. 2. In-plane switching display images obtained from the simulations of a $50 \times 30 \times 10$ lattice with different applied field strengths: $\xi = -1$ (top), $\xi = -3$ (middle), $\xi = -9$ (bottom) at a reduced temperature $T^* = kT/\epsilon = 0.4$.

detailed simulations on these models with, possibly, some more direct connection to actual display simulations.

3. The Optical Images

The intensities resulting from the simulated molecular configurations found, are obtained by means of a Müller matrix treatment as detailed in our papers on TN display[12] and on confined nematic systems.[9–11] To summarize we describe each site in the display by a linear retarder matrix, and the Stokes vector for a light beam that travels through a row of sites across the layers of the display is modified by the matrix resulting from the product of the Müller matrices corresponding to each site. This matrix approach has been also employed in calculations based on continuum theory.[17–19] The light retarded by the spins in the display is observed with the help of crossed polarizers placed on each side of the cell, which switch off the unretarded light obtaining, in such a way, a pixel-by-pixel intensity map $I(x, y)$. The calculation is then repeated over a sufficiently large number (typically 500) of different configurations sampled around a certain evolution step to give the average intensity maps shown with a grey coding in the figures (between black: no light, and white: light through).

In Fig. 2 we show some display images obtained from the visualization procedure and corresponding to Monte Carlo generated configurations of a $50 \times 30 \times 10$ system with different field strengths and using the same refractive and material parameters reported in Ref. 12, even if here we take $\Delta\epsilon < 0$. We see that the display appears as white on black and that it has a better contrast as ξ increases as expected. This confirms that even this relatively small sample can reproduce the basic working of the device. We can then proceed to a more severe test. As mentioned before, a major problem of liquid crystal displays is the variation of brightness and contrast of the optical images when the observer point of view is not perfectly orthogonal to the cell surface.[20]

The viewing angle can be defined using two angular coordinates, θ and ϕ, of a ray vector defined in cartesian coordinates x, y, z as shown in Fig. 3.

To investigate the dependence of the displayed images on the view angle we have considered a $10 \times 10 \times 10$ system where the external field is applied to the two diagonal zones of the fourth layer, subdivided in four regions. Then we have performed a set of simulations varying the angle ϕ for a constant inclination from the vertical $\theta = \pi/8$.

In Fig. 4 we report collectively the results for a Twisted Nematic Display for which the simulations (but not the view angle dependence) have been discussed in a previous paper[12] and the results concerning the present model of in-plane switching effect display.

It is apparent that for this new type of display we have a better resolution at every angle, in comparison with the TN type. The in-plane switching effect display seems to improve this aspect in comparison with the Twisted Nematic one

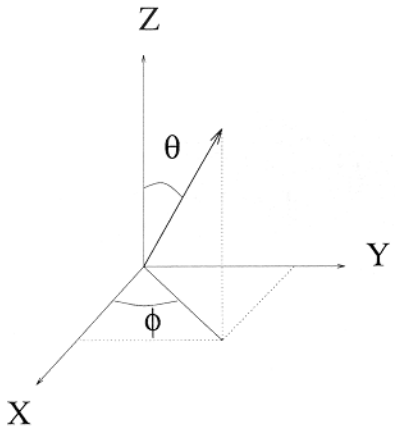

Fig. 3. The angles of view θ and ϕ that define the direction of the observer with respect to the (XY) display plane.

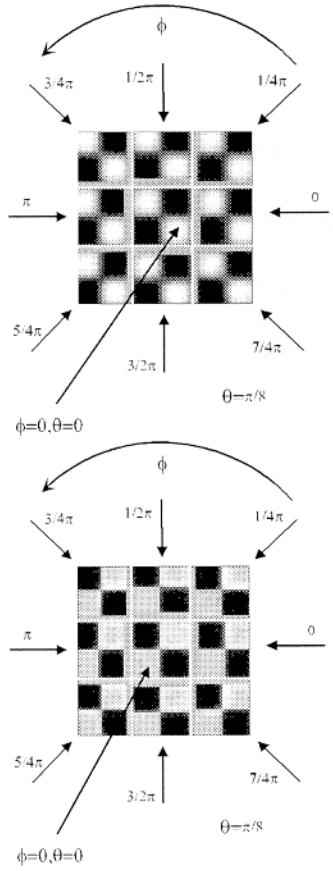

Fig. 4. Simulated optical images obtained, for a constant inclination $\theta = \pi/8$, by varying the viewing angle ϕ of a Twisted Nematic (top) and an In-plane Switching Display (bottom). For each type of display we show nine views identified by the arrows and the corresponding angle ϕ.

although the brightness is lower. Once again our observations are in agreement with experiment[14] and we can proceed to a microscopic level characterization of the device.

4. The Order Parameters

As we have previously shown,[12] one of the most important advantages in using microscopic computer simulations to model liquid crystal displays is the possibility of determining the molecular organization and the ordering at every point across the nematic cell. We remark that these quantities cannot be easily determined by means of other theoretical approaches. In particular we can perform a detailed quantitative investigation of the ordering, introducing and calculating suitable order parameters.

Usually, in simulations of nematic systems the standard second rank order parameter, $\langle P_2 \rangle_\lambda$, is calculated. Considering one layer this can be written as:

$$\langle P_2 \rangle_\lambda^{(L)} = \frac{1}{N_L} \sum_{i=1}^{N_L} P_2(\mathbf{u}_i \cdot \mathbf{d}_L)\,, \tag{2}$$

where N_L is the number of spins belonging to the layer L, $\mathbf{u}_i$ is the vector defining the orientation of the ith spin and $\mathbf{d}_L$ is the local layer nematic director, determined as the eigenvector corresponding to the largest eigenvalue[1,2] of the ordering matrix of the spins of the layer under investigation. The order parameter $\langle P_2 \rangle_\lambda^{(L)}$ expresses how the molecular organization deviates from a perfectly aligned configuration ($\langle P_2 \rangle_\lambda^{(L)} = 1$) but does not indicate where the director is pointing. We have

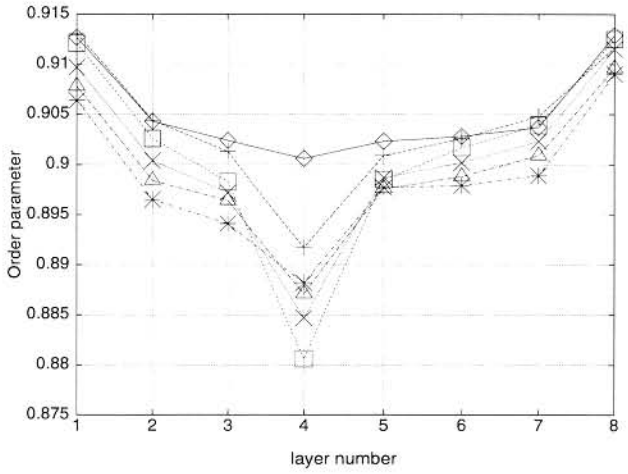

Fig. 5. The second rank nematic order parameter, $\langle P_2 \rangle_\lambda$, calculated at each layer of the cell for a $10 \times 10 \times 10$ lattice at a temperature $T^* = 0.4$. The results correspond to various field strengths: i.e., $\xi = -0.1$ ($\diamond$), $\xi = -0.5$ ($+$), $\xi = -0.9$ ($\square$), $\xi = -1.5$ ($\times$), $\xi = -3.0$ ($\triangle$) and $\xi = -5.0$ ($*$).

studied the $\langle P_2 \rangle_\lambda^{(L)}$ dependence on the intensity of the field applied, ξ, performing a set of independent simulations. The results, as obtained from the simulation of a $10 \times 10 \times 10$ lattice and calculated at each layer of the cell, are shown in Fig. 5. In the present case the external applied field acts on half of the molecules belonging to the fourth fluid layer starting from the bottom. The nematic order parameter $\langle P_2 \rangle_\lambda^{(L)}$, however, expresses the order along the direction of maximum alignment. This is why the difference between the maximum and the minimum of the values reported in Fig. 5 is small, although appreciable. It is also interesting to notice that as the field strength increases the order near the surfaces decreases. This is not true for the calculation performed at the fourth layer, which is the less ordered one, because, at least when the applied field reaches a certain intensity, the ordering is governed by the external coupling.

A more useful indication of the molecular organization stems from the calculation of the order with respect to the field direction at each layer. This *field order parameter* $\langle P_2 \rangle_E^{(L)}$ defined as:

$$\langle P_2 \rangle_E^{(L)} = \frac{1}{N_L} \sum_{i=1}^{N_L} P_2(\mathbf{u}_i \cdot \mathbf{E}), \tag{3}$$

is maximum when all the molecules are directed along the field direction. We can calculate this order parameter in the regions where, referring to the layer where the field is applied, the molecules interact with the external perturbation or not: $\langle P_2 \rangle_E^{(L)\mathrm{ON}}$ and $\langle P_2 \rangle_E^{(L)\mathrm{OFF}}$ respectively. The same calculations can also be performed on the other layers to investigate how the effect of the field propagates across the cell. To do this we have also divided the layers above and below of that one addressed by the field in the same way. We have then calculated $\langle P_2 \rangle_E^{(L)\mathrm{ON}}$ and $\langle P_2 \rangle_E^{(L)\mathrm{OFF}}$ in these regions. The results are summarized in Figs. 6 and 7.

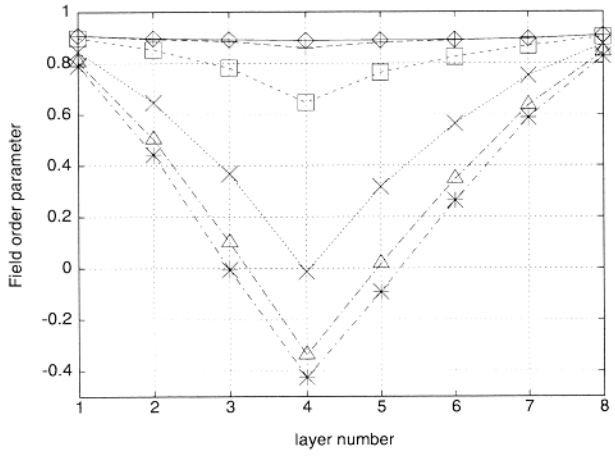

Fig. 6. The field order parameters, $\langle P_2 \rangle_E^{(L)\mathrm{ON}}$ calculated at each layer of a $10 \times 10 \times 10$ cell and for various field strengths. The symbols have the same meaning of Fig. 5.

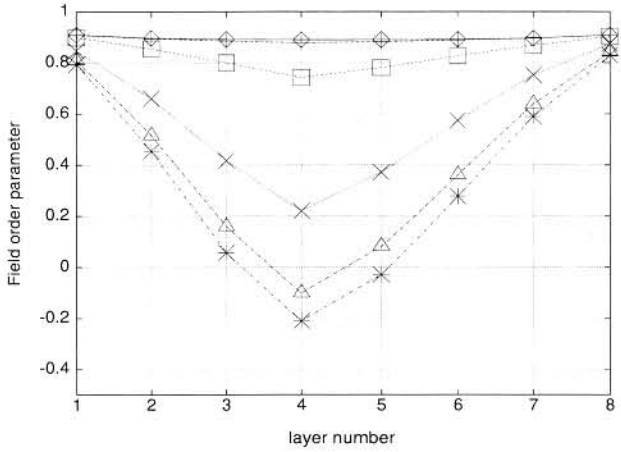

Fig. 7. The second rank order parameter, $\langle P_2 \rangle_E^{(L)\mathrm{OFF}}$, calculated in the regions not directly influenced by the external field.

Looking at Fig. 7 we can verify that upon increasing the field strength the molecules of the layer addressed with the electric field tend to align perpendicularly to the field direction, as expected from their negative dielectric anisotropy. The increase of the field tends to indirectly align also the spins belonging to the other layers, although this effect decreases as the cell surfaces are approached. The calculation of $\langle P_2 \rangle_E^{(L)\mathrm{OFF}}$ shows also that the molecules of the regions are not directly influenced by the field tend to rotate when the coupling is sufficiently high and the curve for $\langle P_2 \rangle_E^{(L)\mathrm{OFF}}$, $\langle P_2 \rangle_E^{(L)\mathrm{ON}}$ are similar from a qualitative, even if not from a quantitative standpoint. Indeed the difference in the minimum value of the field

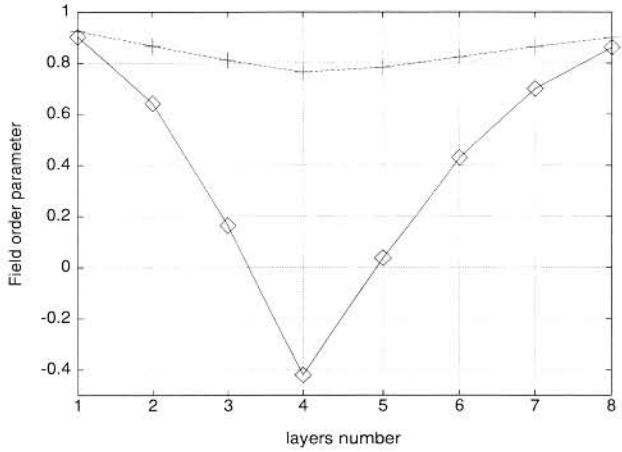

Fig. 8. The field order parameters $\langle P_2 \rangle_E^{(L)\mathrm{OFF}}$ (plus) and $\langle P_2 \rangle_E^{(L)\mathrm{ON}}$ (diamonds) calculated for the larger sample with field strengths $\xi = -9$ and correspondent to the optical image shown in Fig. 2 (bottom).

order parameter can be related to the quality of the optical image. A larger gap should be the measure of better contrast between the black and white zones (see Fig. 8).

5. Conclusions

We have simulated the functioning of an *in-plane switching* liquid crystal display and we have studied its viewing angle dependence, finding it better than that of a *Twisted Nematic* display. These results, similar to those found experimentally, confirm the usefulness and versatility of the Monte Carlo technique that moreover allows the introduction of microscopic level physics not easily accountable with the macroscopic approaches. Indeed Monte Carlo simulations, even when performed on a lattice size like the ones used here, can provide a unique tool for understanding and predicting ordering and microscopic organization point by point. We can also foresee that, using larger systems, the presence of impurities, inhomogeneities and non-ideal surface conditions that constitute prohibitive difficulties for analytical theories should be easily handled with the present approach.

Acknowledgments

C. Z. thanks MURST, University of Bologna and CNR for support. C. C. and P. P. thank INFN for Grant I.S. BO12. We are also grateful to Regione Emilia-Romagna CED for the use of their DEC AXP 7000-710.

References

1. P. A. Lebwohl and G. Lasher, *Phys. Rev.* **A6**, 426 (1972).
2. U. Fabbri and C. Zannoni, *Mol. Phys.* **58**, 763 (1986).
3. Z. Zhang, M. Zuckermann, and O. G. Mouritsen, *Mol. Phys.* **80**, 1195 (1993).
4. C. W. Greef and M. A. Lee, *Phys. Rev.* **E49**, 3225 (1994).
5. C. Chiccoli, P. Pasini, and C. Zannoni, *Int. J. Mod. Phys.* **B11**, 1937 (1997).
6. F. Biscarini, C. Chiccoli, P. Pasini, F. Semeria, and C. Zannoni *Phys. Rev. Lett.* **75**, 1803 (1995).
7. S. Boschi, M. Brunelli, C. Zannoni, C. Chiccoli, and P. Pasini, *Int. J. Mod. Phys.* **C8**, 547 (1997).
8. C. Chiccoli, P. Pasini, F. Semeria, and C. Zannoni, (a) *Phys. Lett.* **150A**, 311 (1990); (b) *Mol. Cryst. Liq. Cryst.* **221**, 19 (1992); (c) *Mol. Cryst. Liq. Cryst.* **212**, 197 (1992).
9. E. Berggren, C. Zannoni, C. Chiccoli, P. Pasini, and F. Semeria, (a) *Phys. Rev.* **E49**, 614 (1994); (b) *Phys. Rev.* **E50**, 2929 (1994); (c) *Mol. Cryst. Liq. Cryst.* **266**, 241 (1995).
10. T. Bellini, C. Chiccoli, P. Pasini, and C. Zannoni, *Phys. Rev.* **E54**, 2647 (1996).
11. C. Chiccoli, O. D. Lavrentovich, P. Pasini, and C. Zannoni, *Phys. Rev. Lett.* **79**, 4401 (1997).
12. E. Berggren, C. Zannoni, C. Chiccoli, P. Pasini, and F. Semeria, *Int. J. Mod. Phys.* **C6**, 135 (1995).
13. G. Baur, R. Kiefer, H. Klausmann, and F. Windscheid, *Liquid Crystals Today* **5**, 13 (1995) and references therein.
14. M. Oh-e and K. Kondo, *Liq. Cryst.* **22**, 379 (1997).

15. N. Metropolis, A. W. Rosenbluth, M. N. Rosenbluth, A. H. Teller, and E. Teller, *J. Chem. Phys.* **21**, 1087 (1953).
16. J. A. Barker and R. O. Watts, *Chem. Phys. Lett.* **3**, 144 (1969).
17. R. Ondris-Crawford, E. P. Boyko, B. G. Wagner, J. H. Erdmann, S. Zumer, and J. W. Doane, *J. Appl. Phys.* **69**, 6380 (1991).
18. F. Xu, H.-S. Kitzerow, and P. P. Crooker, *Phys. Rev.* **A46**, 6535 (1992).
19. A. Kilian, *Liq. Cryst.* **14**, 1189 (1993).
20. P. Bos, *Int. J. Mod. Phys.* **B9**, 2585 (1995).